Soft Matter

PAPER

Electro-creasing instability in deformed polymers: experiment and theory†

Qiming Wang, Mukarram Tahir, Lin Zhang and Xuanhe Zhao*

Subjected to an electric field, a substrate-bonded polymer film develops a biaxial compressive stress parallel to the film. Once the electric field reaches a critical value, the initially flat surface of the polymer locally folds against itself to form a pattern of creases. We show that mechanical deformation of the polymer significantly affects the electro-creasing instability. Biaxially pre-stretching the polymer film before bonding to the substrate greatly increases the critical field for the instability, because the pre-stretch gives a biaxial tensile stress that counteracts the electric-field-induced compressive stress. We develop a theoretical model to predict the critical field by comparing the potential energy of the film at flat and creased states. The theoretical prediction matches consistently with the experimental results. The theory also explains why biaxially pre-stretching a dielectric-elastomer film greatly enhances the measured breakdown field of the film.

1. Introduction

Polymers under voltages have diverse scientific and technological applications including insulating cables, polymer capacitors,[1] surface patternings,[2] polymer actuators,[3,4] tunable optics,[5] energy harvesters,[6] electrocaloric refrigerators,[7] and tactile sensors.[8] Understanding instability of polymers under voltages is not only of practical importance to these applications but also a fundamental topic in physics of soft matter.[9–14] A traditional method for studying the instability is to measure the breakdown electric fields of soft polymers (*e.g.* elastomers and heated polyethylene) and relate the measured fields with the polymers' mechanical properties.[9,15,16] The breakdown fields are regarded as critical fields for the instability, because the instability usually induces electrical breakdown in soft polymers.[4] Although this method has been successful in qualitatively studying the instability and widely used, it has a number of drawbacks. (1) The measured breakdown fields of polymers are generally stochastic due to random factors such as defects in the polymers. In order to obtain a reasonable average value, a large number of tests are required. (2) Because the instability occurs concurrently with electrical breakdown, evolution of the instability cannot be directly observed.[9,10] (3) In most cases, the measured breakdown fields can only be qualitatively related to the postulated mechanism of the instability.[9]

Another method to study the instability is by applying a voltage through an air gap to one or multiple layers of polymers bonded on a rigid substrate.[2,17–20] This method allows the

formation of instability structures in polymers before electrical breakdown. For example, instability patterns of pillars and strips have been observed to form on the polymer surfaces.[2,12,17–21] The air gap is essential in this method, where the permeability difference between air and polymers drives the instability process.[12] Air gaps, however, are mostly avoided in applications of polymers under voltages, because air has a lower breakdown field than most polymers. Therefore, the results from this method usually cannot be directly related to practical applications. In addition, the breakdown of the air gap also limits the maximum applied electric field to a relatively low value (*i.e.* ~10^6 V m^{-1}) in this method.

Recently, we developed a method to directly observe the instability of substrate-bonded polymers under voltages.[22] No air gaps are involved in the experimental setup, so the applied electric field on polymers can rise up to 10^8 V m^{-1} or higher. The key innovation of the method is using a liquid electrode above the polymer and a rigid substrate that bonds on the bottom surface of the polymer as demonstrated in Fig. 1(a). The liquid electrode keeps contact with the deformed polymer, while the rigid polymer substrate prevents the electric field in the deformed polymer from becoming excessively high to avoid electrical breakdown. As illustrated in Video S1†, under a voltage the polymer surface initially maintains a flat state without appreciable deformation. When the voltage reaches a critical value, some regions of the polymer surface suddenly fold upon themselves to form a pattern of creases [Fig. 1(b) and (d)]. As the voltage further increases, the pattern of creases coarsens by increasing their sizes (*i.e.* length and width) and decreasing their density (*i.e.* number of creases per area). This instability is referred to as the *electro-creasing instability*. The measured critical fields for the instability are deterministic, unaffected by random defects in the polymer. The experimental results can be

Soft Active Materials Laboratory, Department of Mechanical Engineering and Materials Science, Duke University, Durham, NC, 27708, USA. E-mail: xz69@duke.edu
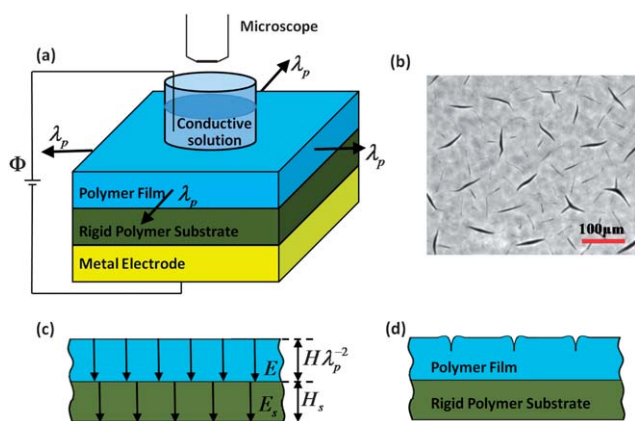
Fig. 1 Schematic illustrations of the current experimental setup for studying the electro-creasing instability (a), a pattern of electro-creases (b), the electric fields in the polymers (c), and a cross-section of the creased film (d).

quantitatively matched with predictions from a theoretical model.

Many polymers under voltages are also mechanically deformed in applications. For example, insulating polymers usually carry mechanical loads from surrounding components and thus deform. As another example, dielectric elastomer is one important type of electro-active polymer actuators.[3,23,24] A milestone in the development of dielectric elastomers is the discovery that the breakdown field of a dielectric elastomer film can be greatly enhanced by pre-stretching the film.[3,25] Although the mechanism for the enhancement is not clear, most of the dielectric-elastomer actuators still work in pre-stretched states.[3,25] In this paper, we will combine experiment and theory to study the electro-creasing instability of deformed polymers bonded on substrates. The work will be further focused on the instability of crosslinked elastomers, which have hyperelastic stress–strain relations. We describe the Experimental methods in Section 2. Section 3 gives Experimental results of critical fields for electro-creasing instability in deformed polymers, and quantitative predictions from theoretical models. In Section 4, we show that the measured breakdown fields of dielectric elastomers are highly possible to be the critical fields of the electro-creasing instability. We further explain why pre-stretching a dielectric-elastomer film increases the measured breakdown field of the film. Section 5 gives the conclusive remarks.

2. Experimental

Fig. 1(a) illustrates the experimental setup to study the electro-creasing instability of deformed polymers bonded on substrates. We chose a two-part silicone elastomer, Ecoflex 00-10 (Smooth-On, USA), as the polymer for the experiment because of its high deformability.[26] The two parts (i.e. base and crosslinker) were mixed, spin-coated on a glass slide covered by Scotch tape (3M, USA), and crosslinked at room temperature for 12 hours. The volume ratio between crosslinker and base was varied from 0.2 : 1 to 1 : 1 to obtain a shear modulus ranging from 5.4 kPa to 10.4 kPa. Ecoflex films of thickness in the range of 227 μm to 724 μm were obtained by varying the spin-coating

speed from 500 rpm to 150 rpm. The shear moduli of the Ecoflex films were measured by uniaxial tensile tests with a Micro-Strain Analyzer (TA Instruments, USA) under a loading rate of 2.5×10^{-4} s^{-1}. The stress–stretch data were fitted to the neo-Hookean model to give the shear moduli of the Ecoflex films. The thicknesses of the un-stretched films were measured by Dektak 150 Stylus Profiler (Bruker AXS, USA).

Following polymerization, the Ecoflex film was peeled off the glass slide and stretched in two orthogonal directions equally by a factor of λ_p as shown in Fig. 1(a). A rigid polymer film, Kapton (DuPont, USA), was bonded on a copper electrode with conductive epoxy (SPI, USA). The stretched Ecoflex film was adhered to the Kapton substrate to preserve the pre-stretch. The top surface of the Ecoflex film was immersed in a transparent conductive solution (20% wt NaCl solution) to permit observing the film's deformation from a microscope (Nikon, Japan) above the solution. The conductive solution also acted as a conformal electrode that keeps contact with the Ecoflex film during its deformation. A high voltage supply (Matsusada, Japan) with controllable ramping rate was used to apply a voltage between the copper substrate and the conductive solution. The ramping rate of the voltage was set to be 10 V s^{-1}. Once the electro-creasing instability appeared on the polymer, the voltage was recorded as the critical voltage.

The breakdown fields of pre-stretched VHB films were measured using the experimental setup demonstrated in Fig. 2 following ref. 27. A VHB film (3M, USA) with a thickness of 500 μm was stretched in two orthogonal directions equally by a factor of λ_p and bonded on a copper substrate. The top surface of the VHB film was immersed in silicone oil (Robinair, USA). A copper rod with a spherical tip of 8 mm in diameter was placed vertically in touch with the VHB film. The rod was also mechanically constrained to avoid any movement during tests. A ramping voltage was applied between the rod and the substrate until electrical breakdown occurred. The breakdown voltages were recorded to calculate the breakdown electric fields.[27] To avoid extremely high voltage, a thinner VHB film (50 μm) was used for the breakdown test of un-stretched film (i.e. $\lambda_p = 1$).

3. Results and discussion

Critical electric field for the instability

The measured critical voltages Φ_c for the electro-creasing instability in films with various thicknesses H and shear moduli
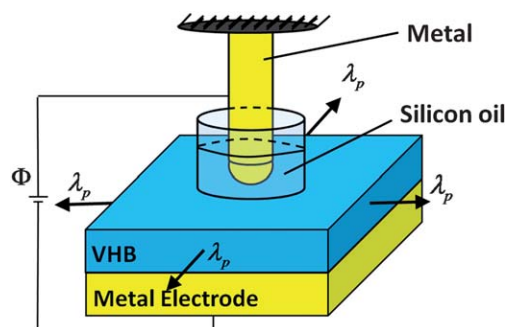

Fig. 2 Schematic illustrations of the current experimental setup for testing the electrical breakdown fields in pre-stretched VHB films.[27]

μ were plotted as functions of the pre-stretch ratio λ_p in Fig. 3(a). The critical voltages strongly depend on the pre-stretch ratio, and their relations are not monotonic. Under the same pre-stretch, Ecoflex films with higher modulus and thickness give higher critical voltages [Fig. 3(a)].

The applied voltage induces electric fields in the Ecoflex film and the Kapton substrate. When the Ecoflex film is in a flat state, the electric fields are normal to the film, as illustrated in Fig. 3(c). Given silicone elastomer is incompressible, the voltage and the electric fields have a relation $\Phi = EH\lambda_p^{-2} + E_s H_s$, where E and E_s are the electric fields in the film and the substrate, and H and H_s the thicknesses of the un-deformed film and the substrate, respectively. Considering the Gaussian law, the electric fields in the film and the substrate are related as $\varepsilon E = \varepsilon_s E_s$, where ε and ε_s are the permittivity of Ecoflex and Kapton, respectively. Therefore, the electric field in the Ecoflex film can be calculated as

$$E = \frac{\Phi}{H\lambda_p^{-2} + H_s \varepsilon/\varepsilon_s} \tag{1}$$

The critical electric fields E_c for the creasing instability can be calculated using eqn (1) with $H_s = 125$ μm, $\varepsilon_s = 3.5\varepsilon_0$, and $\varepsilon = 2.5\varepsilon_0$,[26,28] where the permittivity of vacuum $\varepsilon_0 = 8.85 \times 10^{-12}$ F m^{-1}.
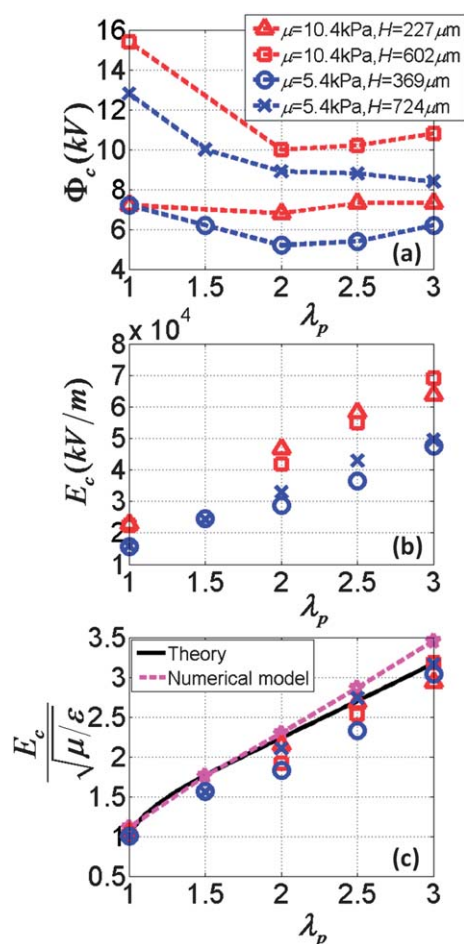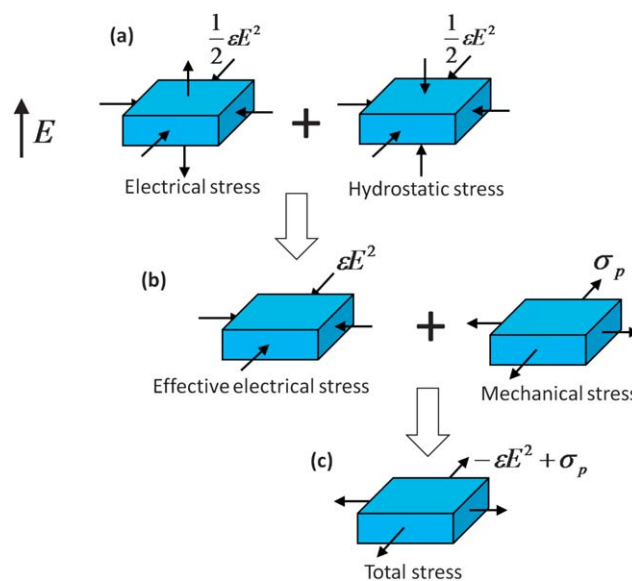
The critical fields are plotted as functions of the pre-stretch ratio in Fig. 3(b). For films with the same modulus but different thicknesses, the critical fields roughly overlap at the same pre-stretch ratio. When the critical fields are further normalized by $\sqrt{\mu/\varepsilon}$ in Fig. 3(c), the normalized values for films with different thicknesses and moduli all collapse onto one single curve. From Fig. 3(b) and (c), it is evident that the biaxial pre-stretch greatly enhances the critical field for the electro-creasing instability.

Previous understanding

Creasing instability has been widely observed on surfaces of soft materials under compression.[29–37] When the compressive stresses in these systems reach critical values, the surfaces of the materials suddenly fold upon themselves to deform into patterns of creases. As discussed in ref. 22, the driving force for the electro-creasing instability is the electric-field-induced compressive stress parallel to the film. Given the dielectric behavior of the Ecoflex film is liquidlike, unaffected by deformation, the electric-field-induced stress can be expressed as[14,38,39]

$$\sigma_{\parallel}^{E} = -\frac{1}{2}\varepsilon E^2; \quad \sigma_{\perp}^{E} = +\frac{1}{2}\varepsilon E^2 \tag{2}$$

The electric field induces a biaxial compressive stress $\sigma_{\parallel}^{E}$ parallel to the film (i.e. perpendicular to the electric field) and a tensile stress $\sigma_{\perp}^{E}$ normal to the film (i.e. along the electric field) as shown in Fig. 4(a). Because the Ecoflex film is regarded as incompressible, superimposing a hydrostatic stress does not affect the deformation of the film. As demonstrated in Fig. 4(a), we superimpose a hydrostatic stress of $-\varepsilon E^2/2$ onto the film to make the total stress normal to the film become zero, so that the mechanical boundary condition is satisfied. This operation results in an effective electrical stress[40]

Fig. 3 The critical voltages (a) and electric fields (b and c) for the electro-creasing instability in polymers with different thicknesses, moduli, and pre-stretch ratios.

Fig. 4 The electrical stress in the film is superimposed by a hydrostatic stress to give an effective electrical stress (a). The effective electrical stress plus the mechanical stress from the pre-stretch (b) gives the total stress in the film (c).

$$\bar{\sigma}_{\parallel}^{\text{E}} = -\varepsilon E^2 \quad (3)$$

in biaxial directions parallel to the film as shown in Fig. 4(b). The effective electrical stress is compressive and increases with the applied electric field. Once the electric field reaches a critical value, the electro-creasing instability occurs.

Theoretical and modeling results

In this paper, we show that biaxially pre-stretching the film before bonding to the substrate increases the critical field for the electro-creasing instability [Fig. 3(c)]. This phenomenon can be qualitatively understood as follows. The pre-stretch induces a biaxial mechanical stress σ_{p} parallel to the film as shown in Fig. 4(b). Therefore, the total stress in the film is the summation of the effective electrical stress and the mechanical stress, *i.e.* [Fig. 4(c)]

$$\sigma = -\varepsilon E^2 + \sigma_{\text{p}} \quad (4)$$

Because the mechanical stress σ_{p} is tensile, the pre-stretch counteracts the effect of the applied electric field on electro-creasing instability. In order to cause the instability in a biaxially pre-stretched film, a higher electric field is needed than in the same film that is not pre-stretched. This is consistent with the experimental results given in Fig. 3(b) and (c).

To calculate the critical electric field for the electro-creasing instability, we compare the potential energies in a region of the film in the stretched and creased states, following the method given in ref. 22, 33 and 41. Because the polymer substrate does not affect the critical field, we neglect the substrate in the calculation. The potential energy in a unit thickness of the region in either flat or creased state [Fig. 5(a) and (b)] can be expressed as[22]

$$\Pi = \int_A W \, \mathrm{d}A + \int_A \frac{1}{2}\varepsilon|E|^2 \, \mathrm{d}A - \int_S \Phi\omega \, \mathrm{d}S \quad (5)$$

where W is the elastic energy density, E is the electric field, Φ is the applied voltage on the surfaces, ω is the surface charge
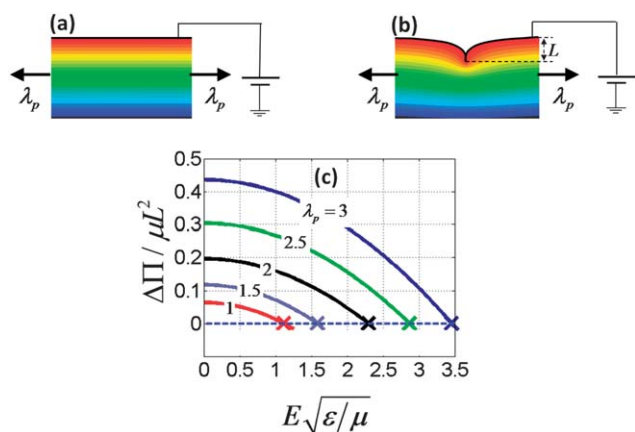
density, and A and S are the area and contour of the region. The first term of eqn (5) gives the elastic energy, and the second and third terms give the electrostatic potential energy of the region. The surface energy of the film has been neglected, because it is orders of magnitude smaller than the elastic energy.[22] By Gaussian law, the charge density on the surface of the film is $\omega = -\varepsilon En$, where n is the surface normal. By substituting ω in eqn (5) and applying divergence theorem and Gaussian law, we can reduce eqn (5) to

$$\Pi = \int_A \left(W - \frac{1}{2}\varepsilon|E|^2 \right) \mathrm{d}A \quad (6)$$

The mechanical tests show that the Ecoflex films obey the neo-Hookean model within a stretch of 3. Therefore, the elastic energy density in eqn (6) is $W = \mu(I - 3)/2$, where $I = \lambda_1^2 + \lambda_2^2 + \lambda_3^2$, and λ_1, λ_2, and λ_3 are the principal stretches. Due to incompressibility of the silicone elastomer, the principal stretches have a relation $\lambda_1\lambda_2\lambda_3 = 1$.

At the flat state, the deformation and electric field are uniform, and thus $\Pi_{\text{flat}} = (W - \varepsilon E^2/2)A$. At the creased state, we analyze the non-uniform deformation and electric field by using finite-element software, ABAQUS 6.10.1, with a user subroutine UMAT.[22] We prescribe a downward displacement L to a line on the top surface of the region, forcing a crease to form as demonstrated in Fig. 5(b).[42] In order to maintain the convergence of the numerical model, we neglect the effect of the electrical stress on the shape of the crease. The region is taken to deform under plain-strain conditions, and only right half of the region is analyzed due to symmetry. The potential energy of the creased state, Π_{crease}, is calculated using eqn (6).

The size of the calculation region is taken to be much larger (100 times) than the size of the crease, so that L is the only length scale relevant in comparing the potential energies in the flat and creased states. The dimensional consideration determines that the potential energy difference has a form[41]

$$\Delta\Pi = \Pi_{\text{crease}} - \Pi_{\text{flat}} = \mu L^2 f\left(E\sqrt{\varepsilon/\mu}, \lambda_{\text{p}}\right) \quad (7)$$

where $f\left(E\sqrt{\varepsilon/\mu}, \lambda_{\text{p}}\right)$ is a dimensionless function of the applied electric field and the pre-stretch ratio. The potential energy difference is plotted as a function of the applied electric field in Fig. 5(c) for various pre-stretches. In the absence of the electric field, the potential energy difference is positive, because $\Pi_{\text{flat}} = 0$ and the elastic energy of the crease gives a positive Π_{crease}. Thus, the flat state is energetically preferable. As the electric field increases, the potential energy difference decreases, because the creased state has a lower electrostatic potential energy than the flat state. Once the electric field reaches a critical value E_{c}, the creased state has the same potential energy as the flat state (*i.e.* $\Delta\Pi = 0$) and the creasing instability sets in.[30,33,41] From Fig. 5(c), we can further see that forming a crease in a film with a higher pre-stretch ratio gives a higher elastic-energy increase from the pre-stretched state. Therefore, a higher electrostatic energy (and thus higher electric field) is required to balance the elastic energy at the higher pre-stretch ratio. As a result, the critical electric field E_{c} increases with the pre-stretch λ_{p}, as shown in Fig. 3(c) and 5(c).

In order to have a semi-analytical expression for the critical field, we assume that the creasing instability occurs when the compressive stress in the film reaches a critical value,

Fig. 5 The equipotential contours in a film at pre-stretched (a) and creased (b) states calculated from the finite-element model. The potential energy difference between the creased and pre-stretched states with various pre-stretch ratios (c).

i.e. $\sigma_c = -\varepsilon E_c^2 + \sigma_p$. The previous analysis gives $E_c \approx 1.03\sqrt{\mu/\varepsilon}$ for $\sigma_p = 0$ (*i.e.* $\lambda_p = 1$),[22] so we can get $\sigma_c \approx -1.06 \mu$. Therefore, the critical electric field for the pre-stretched film can be calculated as

$$E_c \approx \sqrt{\frac{1.06\mu + \sigma_p}{\varepsilon}} \qquad (8)$$

For polymer films that obey the neo-Hookean model, we have $\sigma_p = \mu(\lambda_p^2 - \lambda_p^{-4})$. The critical electric fields calculated with eqn (8) are plotted as functions of the pre-stretch ratio in Fig. 3(c). It can be seen that the theoretical prediction matches well with the experimental and numerical modeling results.

4. Outreach

As discussed in the Introduction, it is well known that the breakdown electric field of a dielectric elastomer film can be greatly enhanced by biaxially pre-stretching the film.[3,25] For example, the measured breakdown field of VHB, the most widely used dielectric elastomer, increases from 18 to 218 MV m^{-1} by a biaxial pre-stretch of 6 times, as shown in Fig. 7(a).[25] The enhancement has been vaguely attributed to factors such as decrease in the defect density by pre-stretch.[3,25] However, it is questionable that these factors alone can give such a huge increase in the breakdown field. Here, we will show that the measured breakdown field of dielectric elastomer is very possible to be the electro-creasing critical field, which can be greatly enhanced by pre-stretch.

A typical experimental setup for measuring the breakdown fields of dielectric elastomers is illustrated in Fig. 6(a).[25] A pair of metal electrodes was clamped around a biaxially pre-stretched film of a dielectric elastomer. The electrodes were mechanically fixed to constrain the deformation of the film. A ramping voltage was applied between the electrodes. Once the electrical breakdown occurred, the voltage was recorded to calculate the breakdown field.

We clamp a brass electrode on a layer of VHB elastomer and observe the electrode–polymer interface under a microscope. It can be seen that air bubbles are easily trapped on the interface as shown in Fig. 6(b). Because air has a breakdown field much lower
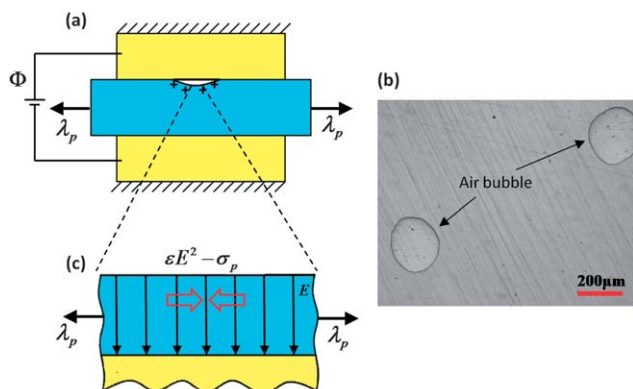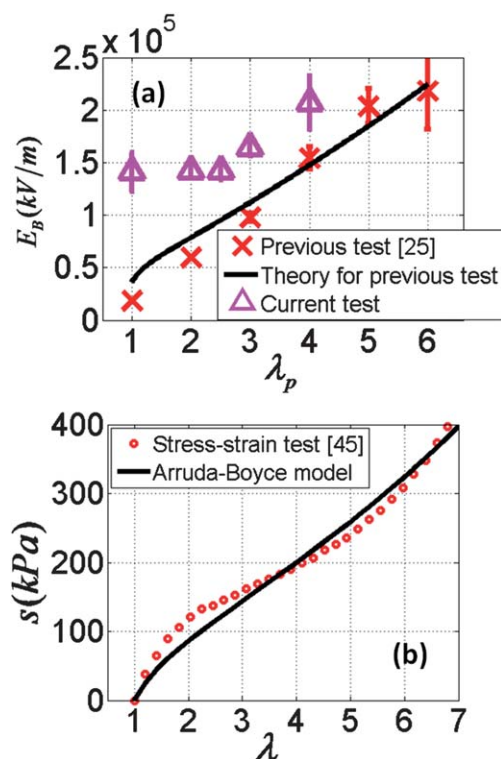
Fig. 7 The breakdown fields of VHB measured with the previous and current methods and the theoretical prediction of results from the previous method[25] (a), and the nominal stress–stretch curve[44] of VHB fitted to the Arruda–Boyce model (b).

than that of the polymer, the air bubbles will be discharged at a lower voltage in the breakdown tests of dielectric elastomers. The discharged air bubbles act approximately as flexible electrodes on the top surface of the polymer film as illustrated in Fig. 6(c).[43] The flexible electrodes allow the electro-creasing instability to develop in regions of the film below the air bubbles, when the electric field reaches a critical value. Since there is no rigid polymer substrate in the experimental setup [Fig. 6(a)], the instability subsequently induces electrical breakdown of the dielectric elastomer and thus the breakdown field is equal to the critical field for the instability,[9,15,16] *i.e.*

$$E_B = E_c \qquad (9)$$

No comment on avoiding air bubbles has been reported in previous breakdown tests of dielectric elastomers.[25] Therefore, it is highly possible that the measured breakdown fields are actually the critical fields for the electro-creasing instability in dielectric elastomer films.

The pre-stretch increases the critical fields of electro-creasing instability in dielectric elastomer films and thus increases the breakdown fields measured with the method illustrated in Fig. 6(a). The critical fields (*i.e.* breakdown fields) can be predicted by eqn (8) with the dielectric and mechanical properties of the dielectric elastomer. The dielectric constant of VHB is $4.5\varepsilon_0$.[25] We plot the nominal stress–stretch relation of VHB measured from a uniaxial tensile test with a stretch rate of 0.094 s^{-1} in Fig. 7(b).[44] In order to account for the stiffening of the polymer at high stretches, the

Fig. 6 The previous experimental setup for measuring the breakdown electric fields of dielectric elastomers[25] (a), and air bubbles trapped on the polymer–electrode interface (b). The discharged air bubbles may induce the electro-creasing instability in the dielectric elastomer (c).

nominal stress–stretch data are fitted to the Arruda–Boyce model $s = \mu(\lambda - \lambda^{-2})(1 + (I/5n) + (11I^2/175n^2) + \ldots)$, where s and λ are the nominal stress and stretch for uniaxial tension, $I = \lambda^2 + 2\lambda^{-1}$, and n is a parameter that accounts for the stiffening effect.[45] By fitting the experimental data in Fig. 7(b), we obtain $\mu = 4.834 \times 10^4$ Pa and $n = 7$. With these parameters, the true stress in the biaxially stretched film can be calculated as

$$\sigma_p = \mu\left(\lambda_p^2 - \lambda_p^{-4}\right)\left(1 + \frac{I}{5n} + \frac{11I^2}{175n^2} + \ldots\right) \qquad (10)$$

where $I = 2\lambda_p^2 + \lambda_p^{-4}$. By substituting eqn (10) in eqn (8), we can predict the breakdown fields for pre-stretched VHB films measured with the method illustrated in Fig. 6(a). From Fig. 7(a), it can be seen that the theoretical prediction matches consistently with the experimental results.

We further measured the breakdown fields of pre-stretched VHB films with the experimental setup illustrated in Fig. 2 following ref. 27. Because the breakdown occurs in a very small area of the film under the spherical tip of the top electrode, the effect of air bubbles is eliminated in the current setup.[27] At least 10 tests were repeated for each pre-stretch ratio, and the mean and standard deviation of the breakdown fields are given in Fig. 7(a). Under the same pre-stretch ratios, the breakdown fields measured with the current method [Δ in Fig. 7(a)] are significantly higher than values from the previous method [$\times$ in Fig. 7(a)]. In addition, the increase in the currently measured breakdown field with pre-stretch [Δ in Fig. 7(a)] is much milder than the previous relation [$\times$ in Fig. 7(a)]. For example, when the pre-stretch increases from 1 to 4, the currently measured breakdown field increases by a factor of 1.47 in contrast to the 8.38 times the increase from the previous test. These results further support the hypothesis that the previously measured breakdown field of dielectric elastomers is the critical electric field of the electro-creasing instability, which can be greatly enhanced by pre-stretch.

5. Conclusion

In summary, we have demonstrated that biaxially pre-stretching a polymer film greatly increases the critical field for the electro-creasing instability, because the pre-stretch gives a tensile stress that counteracts the compressive electrical stress. The increase in the critical field scales with the pre-stretch ratio for a polymer that follows the neo-Hookean law. We have developed a theoretical model to predict the critical field by comparing the potential energy of the film at flat and creased states. The theoretical prediction matches well with the experimental results. We further show that the measured breakdown fields of dielectric elastomers are very possible to be the electro-creasing critical fields, because air bubbles trapped on the elastomer–electrode interface can allow the electro-creasing instability. Therefore, biaxial pre-stretches can greatly enhance the measured breakdown fields of dielectric elastomers. The theoretically predicted critical fields of VHB match consistently with experimentally measured breakdown fields under various pre-stretches. We expect the experimental method and theoretical analysis to have broad applications in studying various modes of instability in polymers under voltages, such as evolution of cavities in polymers under voltages.[46]

References

1 B. J. Chu, X. Zhou, K. L. Ren, B. Neese, M. R. Lin, Q. Wang, F. Bauer and Q. M. Zhang, *Science*, 2006, **313**, 334–336.
2 E. Schaffer, T. Thurn-Albrecht, T. P. Russell and U. Steiner, *Nature*, 2000, **403**, 874–877.
3 R. Pelrine, R. Kornbluh, Q. B. Pei and J. Joseph, *Science*, 2000, **287**, 836–839.
4 X. H. Zhao and Z. G. Suo, *Phys. Rev. Lett.*, 2010, **104**, 178302.
5 Z. H. Fang, C. Punckt, E. Y. Leung, H. C. Schniepp and I. A. Aksay, *Appl. Opt.*, 2010, **49**, 6689–6696.
6 S. J. A. Koh, X. H. Zhao and Z. G. Suo, *Appl. Phys. Lett.*, 2009, **94**, 262902.
7 B. Neese, B. J. Chu, S. G. Lu, Y. Wang, E. Furman and Q. M. Zhang, *Science*, 2008, **321**, 821–823.
8 S. C. B. Mannsfeld, B. C. K. Tee, R. M. Stoltenberg, C. Chen, S. Barman, B. V. O. Muir, A. N. Sokolov, C. Reese and Z. N. Bao, *Nat. Mater.*, 2010, **9**, 859–864.
9 K. H. Stark and C. G. Garton, *Nature*, 1955, **176**, 1225–1226.
10 J. Blok and D. G. Legrand, *J. Appl. Phys.*, 1969, **40**, 288–293.
11 J. C. Fothergill, *IEEE Trans. Electr. Insul.*, 1991, **26**, 1124–1129.
12 V. Shenoy and A. Sharma, *Phys. Rev. Lett.*, 2001, **86**, 119–122.
13 X. H. Zhao and Z. G. Suo, *Appl. Phys. Lett.*, 2007, **91**, 061921.
14 X. H. Zhao, W. Hong and Z. G. Suo, *Phys. Rev. B: Condens. Matter Mater. Phys.*, 2007, **76**, 134113.
15 L. A. Dissado and J. C. Fothergill, *Electrical Degradation and Breakdown in Polymers*, Peter Peregrinus Ltd, London, 1992.
16 X. Zhou, X. H. Zhao, Z. G. Suo, C. Zou, J. Runt, S. Liu, S. H. Zhang and Q. M. Zhang, *Appl. Phys. Lett.*, 2009, **94**, 162901.
17 M. D. Morariu, N. E. Voicu, E. Schaffer, Z. Q. Lin, T. P. Russell and U. Steiner, *Nat. Mater.*, 2003, **2**, 48–52.
18 N. Arun, A. Sharma, P. S. G. Pattader, I. Banerjee, H. M. Dixit and K. S. Narayan, *Phys. Rev. Lett.*, 2009, **102**, 254502.
19 N. Arun, A. Sharma, V. B. Shenoy and K. S. Narayan, *Adv. Mater.*, 2006, **18**, 660–663.
20 S. Y. Chou, L. Zhuang and L. J. Guo, *Appl. Phys. Lett.*, 1999, **75**, 1004–1006.
21 J. Sarkar, A. Sharma and V. B. Shenoy, *Phys. Rev. E: Stat., Nonlinear, Soft Matter Phys.*, 2008, **77**, 031604.
22 Q. Wang, L. Zhang and X. Zhao, *Phys. Rev. Lett.*, 2011, **106**, 118301.
23 P. Brochu and Q. B. Pei, *Macromol. Rapid Commun.*, 2010, **31**, 10–36.
24 Z. Suo, *Acta Mechanica Solida Sinica*, 2010, **23**, 549–578.
25 G. Kofod, R. Kornbluh, R. Pelrine and P. Sommer-Larsen, in *Smart Structures and Materials 2001: Electroactive Polymer Actuators and Devices*, ed. Y. BarCohen, 2001, vol. 4329, pp. 141–147.
26 M. Kubo, X. F. Li, C. Kim, M. Hashimoto, B. J. Wiley, D. Ham and G. M. Whitesides, *Adv. Mater.*, 2010, **22**, 2749–2752.
27 D. B. Watson, W. Heyes, K. C. Kao and J. H. Calderwo, *IEEE Trans. Electr. Insul.*, 1965, **EI–1**, 30–37.
28 Date sheets of Ecofelx 00-10 and Kapton.
29 A. Ghatak and A. L. Das, *Phys. Rev. Lett.*, 2007, **99**, 4.
30 E. Hohlfeld and L. Mahadevan, *Phys. Rev. Lett.*, 2011, **106**, 105702.
31 A. N. Gent and I. S. Cho, *Rubber Chem. Technol.*, 1999, **72**, 253–262.
32 P. M. Reis, F. Corson, A. Boudaoud and B. Roman, *Phys. Rev. Lett.*, 2009, **103**, 045501.
33 S. Cai, K. Bertoldi, H. Wang and Z. Suo, *Soft Matter*, 2010, **6**, 5770–5777.
34 T. Tanaka, S. T. Sun, Y. Hirokawa, S. Katayama, J. Kucera, Y. Hirose and T. Amiya, *Nature*, 1987, **325**, 796–798.
35 H. Tanaka, H. Tomita, A. Takasu, T. Hayashi and T. Nishi, *Phys. Rev. Lett.*, 1992, **68**, 2794–2797.

36 V. Trujillo, J. Kim and R. C. Hayward, *Soft Matter*, 2008, **4**, 564–569.
37 J. Kim, J. Yoon and R. C. Hayward, *Nat. Mater.*, 2010, **9**, 159–164.
38 R. M. McMeeking and C. M. Landis, *J. Appl. Mech.*, 2005, **72**, 581–590.
39 A. Dorfmann and R. W. Ogden, *Acta Mech.*, 2005, **174**, 167.
40 X. H. Zhao and Z. G. Suo, *Appl. Phys. Lett.*, 2009, **95**, 251902.
41 W. Hong, X. H. Zhao and Z. G. Suo, *Appl. Phys. Lett.*, 2009, **95**, 111901.
42 W. H. Wong, T. F. Guo, Y. W. Zhang and L. Cheng, *Soft Matter*, 2010, **6**, 5743–5750.
43 C. Keplinger, M. Kaltenbrunner, N. Arnold and S. Bauer, *Proc. Natl. Acad. Sci. U. S. A.*, 2010, **107**, 4505–4510.
44 J. S. Plante and S. Dubowsky, *Int. J. Solids Struct.*, 2006, **43**, 7727–7751.
45 E. M. Arruda and M. C. Boyce, *J. Mech. Phys. Solids*, 1993, **41**, 389.
46 X. Zhao, S. Cai and Z. Suo, 2011, in preparation.